Analysis of flight parameters and georeferencing of images with different control points obtained by RPA

L.M.D. Santos[1,*], G.A.S. Ferraz[1], M.T. Andrade[1], L.S. Santana[1], B.D.S. Barbosa[1], D.T. Maciel[2] and Giuseppe Rossi[3]

[1]Federal University of Lavras, Department of Agricultural Engineering, University Campus, BR37.200-000 Lavras-MG, Brazil
[2]Federal University of Lavras, Department of Engineering, University Campus, BR37.200-000 Lavras, Brazil
[3]University of Florence, Department of Agriculture, Food, Environment and Forestry (DAGRI), Via San Bonaventura, 13, IT50145 Florence, Italy
*Correspondence: luanna_mendess@yahoo.com.br

Abstract. New techniques for analysing the earth's surface have been explored, such as the use of remotely piloted aircraft (RPA) to obtain aerial images. However, one of the obstacles of photogrammetry is the reliability of the scenes, because in some cases, considerable geometric errors are generated, thus necessitating adjustments. Some parameters used in these adjustments are image overlaps and control points, which generate uncertainties about the amount and arrangement of these points in an area. The aim of this study was to test the potential of a commercial RPA for monitoring and its applicability in the management of and decision-making about coffee crops with two different overlaps and to evaluate geometric errors by applying four grids of georeferenced points. The study area is located in an experimental Arabica coffee plantation measuring 0.65 ha. To capture the images, the flight altitude was standardized to a 30 m altitude from the ground, and a constant travel speed of 3 m s^{-1} was used. The treatments studied were two combinations of image overlap, namely, 80/80% and 70/60%. Six points were tracked through Global Navigation Satellite System (GNSS) receivers and identified with signs, followed by an RPA flight for image collection. The obtained results indicated distinct residual error rates pointing to larger errors along Cartesian axis Y, demonstrating that the point distribution directly affects the residual errors. The use of control points is necessary for image adjustments, but to optimize their application, it is necessary to consider the shape of the area to be studied and to distribute the points in a non-biased way relative to the coordinate axes. It is concluded that the lower overlap can be recommended for use in the flight plan due to the high resolution of the orthomosaic and the shorter processing time.

Key words: orthorectification of images, geometric error, photogrammetry, UAS (Unmanned Aircraft System), overlap.

INTRODUCTION

Photogrammetry consists of the analysis of a terrestrial surface strip using a set of aerial photographs, providing the observer with information about the objects on the land surface and a safe way to analyse the environment. According to Moriya (2015), remote

sensing and photogrammetry products have great potential for use in precision agriculture, encouraging the development of new methodological approaches and applications that produce good spatial information to support rural farmers in crop planning and decision-making.

To facilitate classical photogrammetry, new technologies have been tested, such as the use of remotely piloted aircraft (RPA). The use of RPA in precision agriculture can help rural farmers identify management strategies, supporting measures to increase efficiency in the management of the production process, maximizing crop yields, and reducing input costs, thus making this activity more competitive (Oliveira et al., 2007; Silva et al., 2008; Carvalho et al., 2009). These platforms are being studied and used to obtain images with a high temporal resolution (for example, acquired several times a day), high spatial resolution (in centimetres and even millimetres), and low operating costs (Lelong et al., 1998; Hunt et al., 2005; Nebiker et al., 2008; Rango et al., 2009; Hardin & Hardin, 2010; Laliberte & Rango, 2011; Xiang & Tian, 2011; Honkavaara et al., 2013; Torres-Sánchez et al., 2014). They can be applied in smaller areas and in specific locations for obtaining data in less time, accompanying the growth of several crops, for example.

In addition, photogrammetry and remote sensing stand out due to the speed and quality of the data obtained, as indicated by Volterrani (2003), enabling the use of remote images to identify plant species; to calculate leaf areas, biomass and soil cover; and even to quantify levels of nitrogen, chlorophyll, water or nutritional deficiencies. The use of aerial images has emerged as a promising alternative since they are already used in agriculture for mapping crops, evaluating cultivated areas, and detecting different types of deficiencies (Molin, 2015).

Although RPA has built-in GPS, its accuracy is not high enough for direct geo-referencing, requiring soil control points (GCPs) (Chang et al., 2017). Thus it is necessary to use referenced points for in order to obtein a corect georeferencing in projects that require good geometric precision, such as the generation of a digital terrain model (DTM), planting rows monitoring, monitoring crop growth and obtaining information for field interventions. According to Zanetti et al. (2017), GCPs are necessary to ensure accuracy in the generation of orthophotos and can directly influence the positional quality of the products generated. GCPs can greatly increase the accuracy of maps, and these control points can either be marked on the ground or be landmarks such as the intersections of roads or the corners of buildings that can be identified in the image (Wang et al., 2012). According to Agüera-Vega et al. (2017) at least three GCPs are needed for this process, but it is recommended to use significantly more to reach better accuracies.

The flight parameters used when obtaining images such as the overlap, height, and speed may affect the quality and accuracy of the orthomosaic. Studies carried out by Mesas-Carrascosa et al. (2016) show that the overlap is a factor that can affect the accuracy and quality of the final product. The authors tested two configurations of longitudinal and transverse overlaps (80%–50% and 70%–40%) and found that the highest overlap (longitudinal 80% and transverse 50%) was the most recommended for creating the orthomosaic. However, depending on the purpose and final product, larger overlaps will increase the capture time of the images, which will result in a larger number of point clouds and, consequently, a longer processing time. Therefore, whether there is a need for a high amount of overlap for an intended purpose should be studied and

evaluated. Siebert & Teizer (2014) recommend using longitudinal and transverse coverage areas of at least 70 and 40%, respectively.

In this context, overlap for coffee crop analysis and the number of GCPs to be used in a given area is still unknown, requiring accurate and precise data from aerial images processed with different GCPs.

The aim of the present work was to test the potential of a commercial RPA for monitoring and applicability in the management of and decision-making about coffee crops with two different overlaps and to evaluate geometric errors by applying four grids of georeferenced points.

MATERIALS AND METHODS

The study was carried out at the Federal University of Lavras (UFLA) (Fig. 1), in the city of Lavras, Minas Gerais, Brazil. The study site comprises 0.65 hectares of an experimental area at 21°13'33.23" South latitude, 44°58'17.63" West longitude. A área de estudo é considerada um terreno plano
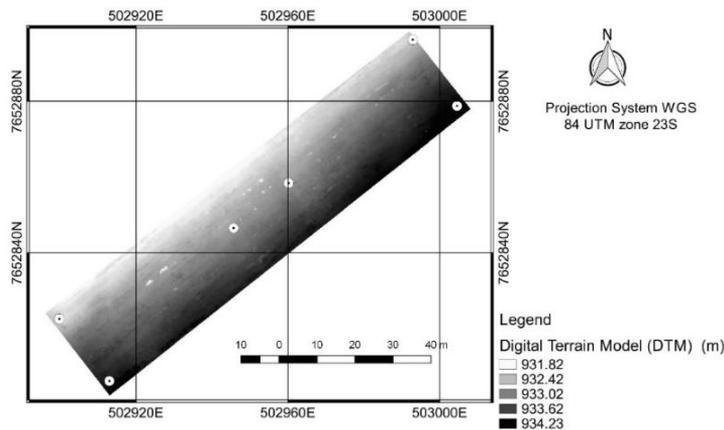

Figure 1. Digital model of elevation of the study area and distribution of control points.

The study site is the remnant area of an experiment described by Caldas et al. (2018) and was established in February 2009 with *Coffea arabica* L., cultivar Travessia, with 2.60×0.60 m spacing, totalling 36 blocks with 3 planting rows and 14 plants per row. The coffee plants were pruned ('esqueletamento') in the third week of July 2016. According to Queiroz-Voltan et al. (2006), 'esqueletamento' is considered a drastic pruning that consists of removing a large part of the plagiotropic branches, approximately 20 cm at the top, and ending with 40 cm in the low plagiotropic branches, with the recovery of production in around one year. In 2017, the irrigation and fertigation treatments were not applied, although there was likely a residual effect from the previous fertilization.

In this area, 6 GCPs were pre-defined and were fixed and tracked in the field using a pair of Global Navigation Satellite System (GNSS) devices with Real Time Kinematics (RTK), composed of a base and rover, and the Spectra Precision SP60 model with the following characteristics: 240-channel receptors operating at frequencies C/A, L1, L2 and L3 and in kinematic mode (RTK). Data were processed to improve data quality.

Four points were collected at the extremes of the area and two points in the middle of the area. The rover rod was 2.0 m high, the height of the coffee trees ranged from 1.80 to 2.10 m, with no multi-streaming effect. The collections were made on the floor, on the control plates fixed to the floor. The points were fixed to the field in the RTK mode with accuracy of 0.03 m, if there were the distance between the base and the rover, it would be corrected with the longest follow-up time. Thus, the distance between the points and the base was small to consider the effect of the distance on the errors.
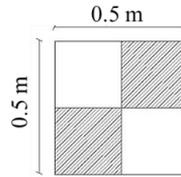
Figure 2. Control point model for characterization of the georeferenced points.

An identification sign was placed on each tracking site (Fig. 2 and Table 1) for identification in the images obtained by RPA.

Table 1. Description of the control points and their distance from the base of the GPS RTK

| GCP	North (m)	East (m)	Altitude (m)	Point Distance With RTK Base (m)
1	7652806.21	502913.00	931.45	67.81
2	7652822.58	502899.8	929.78	79.00
3	7652846.57	502945.72	930.46	40.98
4	7652858.42	502960.23	930.42	40.52
5	7652896.29	502992.93	929.83	75.19
6	7652878.80	503004.58	931.61	61.97

An RPA DJI Phantom 3 Professional was used, which is a four-bladed rotary-wing aircraft with four battery-powered motors, vertical landing and take-off, 23 minute flight autonomy, a gimbal for camera stabilization, and damping of vibrations and correction of camera orientation when taking photos. It is oriented perpendicular to the ground, has an integrated Global Positioning System (GPS), and is operated by remote control. It has a coupled Sony digital camera, model EXMOR 1/ 2.3", with 12 megapixel resolution, obtaining images in true colour (red R, green G, blue-B) and 8-bit radiometric resolution; the camera has a 20 mm lens with an f/2.8 aperture and a maximum image resolution of 4,000 × 3,000 pixels, and its photos are stored on an SD card.

To capture the images, the flight height was standardized to an altitude of 30 m from the ground with a constant travel speed of 3 m/s, with two combinations of forward and side overlaps, namely, 80/80% and 70/60%.

For processing the images and creating the orthomosaics, PhotoScan software from Agisoft Pro version 1.4.4 (Agisoft LLC, St. Petersburg, Russia) was used. This software identifies homologous points in the images, forming a dense point cloud, thus enabling the reconstruction of the model and the creation of the orthomosaic as a final product. The orthomosaic was exported in GEOTIFF format and later processed on GIS software. The GCPs were analysed with the highest overlap, 80/80%, to ensure the accuracy and quality of the final product.

The GCPs obtained from the GNSS tracking were divided into three sets of 4, 5, and 6 points, as shown in Fig. 3. The georeferencing was performed as follows: linear transformation and re-sampling method, coordinate reference system SRC, SIRGARS 2000 UTM and zone 23 south. Then, the points were adjusted manually, informing the

software of the locations of the points and generating an accuracy report that contained the residual errors of each adjusted point. Fig. 3 shows the conformation of how the tracking was performed and the final product of the georeferencing of the images.
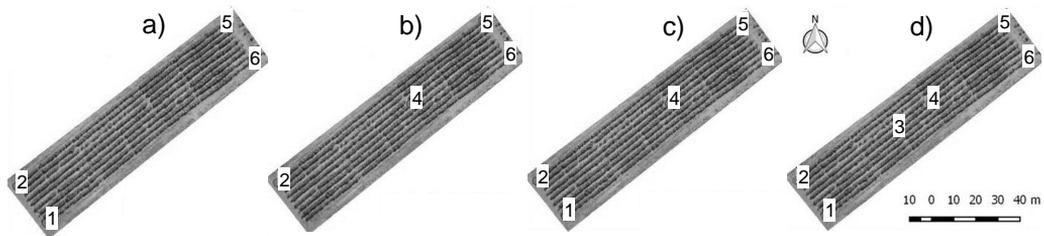
Figure 3. Locations of georeferenced GCPs: a) 4 points; b) 4 points with a centre point; c) 5 points; d) 6 points.

RESULTS AND DISCUSSION

From the image processing, and with the orthomosaics observed in Fig. 4 as the end result, it was possible to analyse the generated images. The evaluation of the two overlaps reveals the presence of invasive plants in the canopies of some of the coffee plants. In addition, with the analysis of the images, it is possible to characterize the crop uniformity, with the northeast region of the area displaying a block of uneven coffee plants, in addition to detecting the planting and alignment gaps.
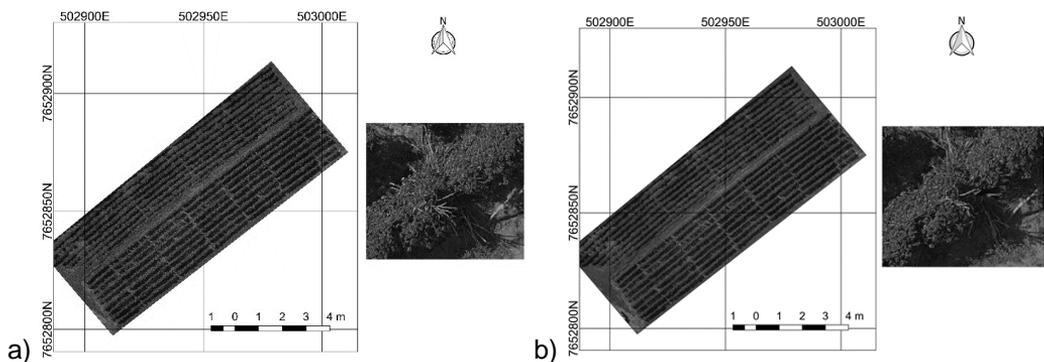
Figure 4. Ortomosaics obtained through field image processing with vertical / horizontal overlap of (A) 80/80% and (A) 60/70% respectively.

From the results, it is justifiable to use RPA as a tool for guiding crop management practices with greater assertiveness in the field, citing as an example the uses of agricultural inputs at variable rates. Castaldi et al. (2016), who carried out the mapping of invasive species for the targeted application of herbicides in a corn crop, concluded that the use of post-emergence image data obtained by RPA led to a decrease in herbicide use, increasing the untreated areas from 14% to 39.2% for uniform spraying and from 16 to 45 € ha. This fact justifies the adoption of such technologies in the coffee crop.

Analysing the data described in Table 2, as well as the results of the image processing, it is possible to conclude that the resolution of the images is lower than 1.5 cm pixel^{-1}.

From the parameters observed in Table 2, it is possible to infer that the spatial resolutions observed in the field images are very close, with a difference of only 0.02 cm/pixel, which is a negligible value for the purpose of the present evaluation. Another relevant point is the flight time for each of the observed overlaps, in which the 70/60% overlap leads to a 26.9% shorter flight time of the RPA for collecting the images for the same area.

Table 2. Result of the image processing, demonstrating the evaluated flight parameters for the two image overlaps

Overlap (%)	Image evaluation parameters			
	Flight time (min)	Number of Images	Processing time (h)	Space Resolution (cm pixel^{-1})
80×80	7.88	93	4.79	1.31
70×60	5.76	90	4.88	1.33
Fixed flight parameters				
Velocity (m s^{-1})	3.0			
Flight height (m)	30			

Regarding the processing time, it is known that images collected with a high overlap generate more points and that the cloud is one of the processing procedures that requires the most time; such processes are differentiated by the quantity of the images and the quality of the product. However, a higher-quality procedure results in a higher quality of the model generated. For both overlaps evaluated, high-quality parameters were used, both of which resulted in high-quality products. Therefore, there was no significant difference in the processing time, which was 0.09 hours or slightly more than 5 minutes.

Obtaining images with a low overlap, less than that recommended by photogrammetry (60/30%), may affect the accuracy and quality of the final product and the estimates (Mesas-Carrascosa et al., 2016). The overlap is a factor that must be taken into account, as it may compromise the analyses of the biophysical parameters of crops, as observed in studies by Haas et al. (2016), where the authors used a 60/60% overlap and obtained a non-homogeneous point density and data holes, due to the low overlap and consequently few points in the dense cloud, which hinders model construction, causing gaps in the images. Dandois et al. (2015) used an 80% overlap with good accuracy, and Guerra-Hernández et al. (2017) used an 80% longitudinal overlap and 75% lateral overlap and obtained good results. The greater the overlap was, the greater the number of points in the point cloud the consequently longer the processing time and the hardware and software demand to support such processing.

Chang et al. (2017) used overlays with 90% frontal and lateral overlap, the authors state that source error may include uncertainties in DTM generation, inaccurate geo-spatial data product geo-referencing and unstable data acquisition conditions. These uncertainties in the generation of DTMs include flight planning and its features such as overlap, flight height, flight speed, as well as the quality of processing of these images.

Another parameter that can be discussed is the flight height of the aircraft, which in this case for both overlaps evaluated was 30 m. The flight height of the RPA is directly

related to the spatial resolution of the images. In this situation, due to the height of the aircraft being very close to the target, it allowed greater detail of the crop, which had a positive effect on the final products generated in the processing. In studies carried out by Romero et al. (2015), the authors obtained a spatial resolution of 10 cm using an RPA model Phantom 2, with a flight height of 120 m, that is, the spatial resolution and the coverage of the area are directly affected by the flight height.

The visual displacement of the tacked point relative to the georeferenced point is observed in Fig. 5. This shows the need for adjustments in the obtained images, as the square should have been overlapped with the circle.
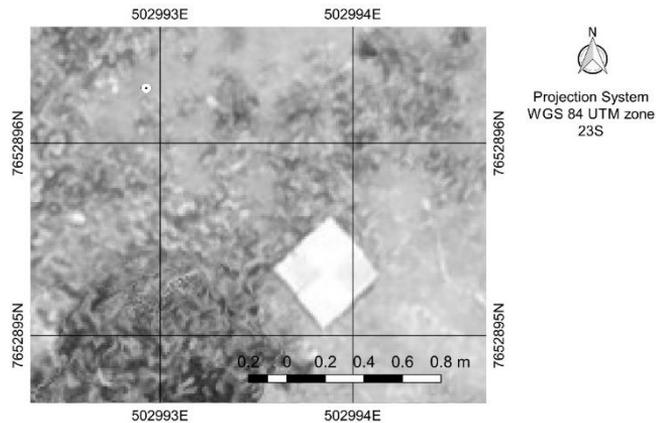
Figure 5. Error found before the georeferencing of images. The circle represents the point tracked through GNSS, and the square is a point that was visualized by the RPA.

As observed in Table 3, the field-tracking data in RTK mode indicates the high reliability of the tie points, showing an accuracy between 0.014 and 0.024 m. These standard deviation rates are indicative of a high accuracy. According to the standard NBR 13133 (1994), GNSSs are considered to be highly accurate electronic distance metres (EDM), as they reach minimum errors of 3 mm.

Tahar & Ahmad (2013) studied the GCPs on a area of 150 ha and observed that any number and distributions of GCPs studied, as in this work, the horizontal accuracy was better than the vertical one.

Table 3. Results of the reports resulting from post-processing adjustments of the field data collected through GNSS in RTK mode

Vector ID	Type of solution	Precision H (m)	Precision V (m)
1	Fixo	0.017	0.024
2	Fixo	0.021	0.029
3	Fixo	0.014	0.022
4	Fixo	0.021	0.027
5	Fixo	0.017	0.027
6	Fixo	0.019	0.027

From the analysis in Table 4, it is possible to observe the residual errors in metres, indicating the differences between the points tracked by the GNSS and the points visualized by the RPA, that is, the displacement of the coordinates in metres obtained in both systems. When analysing the average error, the arrangement with 4 points located at the vertex of the area was the most advantageous of the conformations, which may have been due to the small size of the area studied, responding better to the points in the vertices only.

Table 4. Residual errors in metres of the UTM coordinates "X and Y"

ID	4 points		4 points A		5 points		6 points	
	Res X	Res Y	Res X	Res Y	Res X	Res Y	Res X	Res Y
1	-	-	3.83	-6.16	4.33	-8.94	4.58	-10.77
2	1.77	0.42	-3.03	4.27	-1.74	9.03	-0.96	10.52
3	-	-	-	-	-	-	0.45	4.09
4	-4.11	-8	-	-	-4.46	-2.92	-7.72	-6.88
5	-0.36	-9	-2.85	-12.14	-1.44	-11.82	-0.36	-11.8
6	2.69	17	2.06	14.03	3.32	14.64	4	14.84
Mean error	2.23	8.60	2.94	9.15	3.05	9.47	3.011	9.81

The results indicate that the latitude (Y) coordinates are the ones with the highest errors, generating high residual error rates. Fig. 3, b (3 points in the vertex and one central point) and Fig. 3, d (6 points), 17 and 14.84 m, respectively, showed that the residual values of (Y) are better in the conformation represented in Fig. 3, a (4 points located at the vertices of the area), with better results when the points are positioned at the vertices. This indicates the influence of the position of the points in the area and may complement the recommendations of Pix4d, which stipulate only a minimum of 5 control points for small surface areas and recommends 5 to 10 control points for large projects.

At the longitude points (X), the values are relatively low relative to the (Y) axis, making it clear that the shape of the area influences the residual errors of the GCPs, since the smaller distances are on the (X) axis, indicating that the clustering of the points improves the residual errors. However, this work reaches results different from those found by Tahar & Ahmad (2013) and Perin et al. (2016), who concluded that the higher the number of points, the greater the accuracy. Although the number of points is important, the results show the high level of significance of the clustering and distribution of points and the size of the area studied.

Studies by Wallace et al. (2016) used 24 targets as GCPs collected with dual-frequency RTK GPS in a 30×50 m area, obtaining a position error within ± 0.05 m horizontally and ± 0.20 m vertically. Turner et al. (2015) collected 23 GCPs with a dual-frequency GPS RTK in an area of 125×60 m and obtained position errors of approximately 0.04–0.05 m horizontally and 0.03–0.04 m vertically. Both authors used a small area with a considerable amount of points, however the present study had good results using a minimum number of points when they were scattered in the study area.

CONCLUSIONS

It was possible to test the use of a commercial RPA using two different flight plans in a coffee crop area. The presence of weeds both in between the planting rows and in the coffee canopy, gaps in the planting, and the alignment and uniformity of the crop in both overlaps studied were identified.

It was also concluded that the number of GCPs for the area evaluated did not alter the accuracy but did alter the distribution of the points. The evaluation of the geometric errors for the study area showed the importance of the distribution of the GCPs and that their clustering or distance can have an isolated effect on each coordinate axis evaluated. The study showed that for the better development of this application, it is important to

consider the shape of the study area and to distribute the points in a scattered and non-biased way relative to the coordinate axis.

REFERENCES

Agüera-Vega, F., Carvajal-Ramírez, F. & Martínez-Carricondo, P. 2017. Assessment of photogrammetric mapping accuracy based on variation ground control points number using unmanned aerial vehicle. *Measurement* **98**, 221–227.

Caldas, A.L.D., Lima, E.M.C., Rezende, F.C., Faria, M.A.D., Diotto, A.V. & Júnior, M.C.R.L. 2018. Yield and quality of coffee cv. Travessia under different irrigation and phosphate fertilization. *Revista Brasileira de Agricultura Irrigada* **12**, 2357–2365 (in Portuguese).

Carvalho, G.R., Botelho, C.E., Bartholo, G.F., Pereira, A.A., Nogueira, Â.M. & Carvalho, A.M. 2009. Behavior of F4 progenies obtained by 'Icatu' crosses with 'Catimor'. *Ciência e Agrotecnologia* **33**, 47–52 (in Portuguese).

Castaldi, F., Pelosi, F., Pascucci, S. & Casa, R. 2016. Assessing the potential of images from unmanned aerial vehicles (UAV) to support herbicide patch spraying in maize. *Precision Agriculture* **18**, 76–94.

Chang, A., Jung, J., Maeda, M.M. & Landivar, J. 2017. Crop height monitoring with digital imagery from Unmanned Aerial System (UAS). *Computers and Electronics in Agriculture* **141**, 232–237.

Dandois, J.P., Olano, M. & Ellis, E.C. 2015. Optimal altitude, overlap, and weather conditions for computer vision UAV estimates of forest structure. *Remote Sensing* **7**, 13895–13920.

Guerra-Hernández, J., González-Ferreiro, E., Monleón, V.J., Faias, S.P., Tomé, M. & Díaz-Varela, R.A. 2017. Use of Multi-Temporal UAV-Derived Imagery for Estimating Individual Tree Growth in Pinus pinea Stands. *Forests* **8**, 300–319.

Haas, F., Hilger, L., Neugirg, F., Umstaedter, K., Breitung, C., Fischer, P. & Schmidt, J. 2016. Quantification and analysis of geomorphic processes on a recultivated iron ore mine on the Italian island of Elba using long-term ground-based lidar and photogrammetric SfM data by a UAV. *Natural Hazards and Earth System Sciences* **16**, 1269–1288.

Hardin, P.J. & Hardin, T.J. 2010. Small-scale remotely piloted vehicles in environmental research. *Geography Compass* **4**, 1297–1311.

Honkavaara, E., Saari, H., Kaivosoja, J., Pölönen, I., Hakala, T., Litkey, P. & Pesonen, L. 2013. Processing and assessment of spectrometric, stereoscopic imagery collected using a lightweight UAV spectral camera for precision agriculture. *Remote Sensing* **5**, 5006–5039.

Hunt, E.R., Cavigelli, M., Daughtry, C.S.T., Mcmurtrey, J.E. & Walthall, C.L. 2005. Evaluation of digital photography from model aircraft for remote sensing of crop biomass and nitrogen status. *Precision Agriculture* **6**, 359–378.

Laliberte, A.S. & Rango, A. 2011. Image processing and classification procedures for analysis of sub-decimeter imagery acquired with an unmanned aircraft over arid rangelands. *GIScience e Remote Sensing* **48**, 4–23.

Lelong, C.C.D., Pinet, P.C. & Poilve´, H.1998. Hyperspectral imaging and stress mapping in agriculture: A case study on wheat in Beauce (France). *Remote Sensing of Environment* **66**, 179–191.

Mesas-Carrascosa, F.J., Notario García, M.D., Meroño De Larriva, J.E. & García-Ferrer, A. 2016. An Analysis of the Influence of Flight Parameters in the Generation of Unmanned Aerial Vehicle (UAV) Orthomosaicks to Survey Archaeological Areas. *Sensors* **16**, 1838–1852.

Molin, J.P., do Amaral, L.R. & Colaço, A. 2015. *Precision Agriculture (Agricultura de precisão)*. São Paulo, Brazil, 224 pp. (in Portuguese).

Moriya, E.A.S. 2015. *Identification of spectral bands to detect healthy and diseased sugarcane using hyperspectral camera on board UAV*. Doctoral Thesis. UNESP. (in Portuguese)

NBR, ABNT. 13133-1994. *Execution of topographic survey: procedure*. Rio de Janeiro.

Nebiker, S., Annen, A., Scherrer, M. & Oesch, D. 2008. A light-weight multispectral sensor for micro UAV: Opportunities for very high resolution airborne remote sensing. *The International Archives of the Photogrammetry, Remote Sensing and Spatial Information Sciences* **37**, 1193–1200.

Oliveira, E.D., Silva, F.M.D., Guimarães, R.J. & Souza, Z.M.D. 2007. Elimination of lines in coffee beans with semi-mechanized. *Ciência e Agrotecnologia* **31**, 1826–1830 (in Portuguese).

Perin, G., Gerke, T., Lacerda, V.S., da Rosa, J.Z., Caires, E.F. & Guimarães, A.M. 2016. Accuracy Analysis of Georeferencing of Mosaics of Images Obtained by RPA. Anais do EATI-Encontro Anual de Tecnologia da Informação e STIN–*Simpósio de Tecnologia da Informação da Região Noroeste do RS, Rio Grande do Sul*, pp. 193–199 (in Portuguese).

Queiroz-Voltan, R.B., Perosin Cabral, L., Paradela Filho, O. & Fazuoli, L.C. 2006. Efficiency of pruning in coffee trees in the control of Xylella fastidiosa. Bragantia, Campinas, **65**, pp. 433–440 (in Portuguese).

Rango, A., Laliberte, A., Steele, C., Herrick, J.E., Bestelmeyer, B., Schmugge, T. & Jenkins, V. 2006. Using unmanned aerial vehicles for rangelands: current applications and future potentials. *Environmental Practice* **8**, 159–168.

Romero, V.R., Villareal, A.M., León, J.L.T. & Hernández, A.H. 2015. Perspectives of UAV technology in oil palm cultivation: crop monitoring using high resolution aerial images. *Revista Palmas* **36**, 25–41 (in Spanish).

Siebert, S. & Teizer, J. 2014. Mobile 3D mapping for surveying earthwork projects using an Unmanned Aerial Vehicle (UAV) system. *Automation in Construction* **41**, 1–14.

Silva, F.M.D., Souza, J.C.S.D. & Alves, M.C. 2008. Influence of manual harvest in the spatial variability of coffee yield and defoliation along two agricultural harvests. In: *International Conference of Agricultural Engineering*, Foz do Iguaçu (in Portuguese).

Tahar, K. & Ahmad, A. 2013. An evaluation on fixed wing and multi-rotor UAV images using photogrammetric image processing. *International Journal of Computer, Electrical, Automation, Control and Information Engineering* **7**, 48–52.

Torres-Sánchez, J., Peña, J.M., Castro, A.I.D. & López-Granados, F. 2014. Multi-temporal mapping of the vegetation fraction in early-season wheat fields using images from UAV. *Computers and Electronics in Agriculture* **103**, 104–113.

Turner, D., Lucieer, A. & de Jong, S. 2015. Time series analysis of landslide dynamics using an unmanned aerial vehicle (UAV). *Remote Sensing* **7**, 1736–1757.

Volterrani, M. 2003. Effects of nitrogen nutrition bermudagrass spectral reflectance. *International Turfgrass Society* **10**, 1005–1014.

Wallace, L., Lucieer, A., Malenovský, Z., Turner, D. & Vopěnka, P. 2016. Assessment of forest structure using two UAV techniques: A comparison of airborne laser scanning and structure from motion (SfM) point clouds. *Forests* **7**, 1–16.

Wang, J., Ge, Y., Heuvelink, G.B., Zhou, C. & Brus, D. 2012. Effect of the sampling design of ground control points on the geometric correction of remotely sensed imagery. *International Journal of Applied Earth Observation and Geoinformation* **18**, 91–100.

Xiang, H. & Tian, L. 2011. Method for automatic georeferencing aerial remote sensing (RS) images from an unmanned aerial vehicle (UAV) platform. *Biosystems Engineering* **108**, 104–113.

Zanetti, J., Junior, J.G. & Santos, A.D.P.D. 2017. Influence of number and distribution of control points on orthophotos generated from a survey by vant. *Revista Brasileira de Cartografia* **69**, 263–277 (in Portuguese).